PSI-SR-1175

Re-Entry Plasma Induced Pseudorange and Attenuation Effects in a GPS Simulator

Donald S. Frankel
Peter E. Nebolsine
Merlin G. Miller
James M. Glynn

Donald S. Frankel, Peter E. Nebolsine, Merlin G. Miller, James M. Glynn, "Re-Entry Plasma Induced Pseudorange and Attenuation Effects in a GPS Simulator ," presented at SPIE Defense and Security Symposium (Orlando, FL), *SPIE Proceedings* **5420** (12-16 April 2004).

Re-entry plasma induced pseudorange and attenuation effects in a GPS simulator

Donald S. Frankel*, Peter E. Nebolsine, Merlin G. Miller, and James M. Glynn
Physical Sciences Inc., 20 New England Business Center, Andover, MA 01810

ABSTRACT

Physical Sciences Inc. (PSI) is developing, with Navy SBIR Phase II funding, a hardware in the loop Global Positioning System (GPS) receiver Testbed. A computer simulation will "fly" a re-entry body (RB) along its trajectory and compute plasma properties that produce GPS signal attenuation and pseudo-range changes for each GPS satellite in view for the specified day and time. (The specified day and time determine the locations of the GPS satellites relative to the RB.) The simulation will compose digital instructions that specify GPS signal attenuation and pseudo-range change. The instructions will be sent to a GPS signal simulator via Ethernet using UDP. The GPS signal simulator generates analog RF electronic signals that are fed into a real, physical GPS receiver, thus emulating what would occur on an RB in flight. The GPS receiver navigational output will be compared to the input trajectory to determine the accuracy of the GPS receiver. Because attenuation of the GPS satellite signals will be, in general, different for each satellite, the effect of sequential loss of signal from various GPS satellites and the degradation on GPS trajectory determination will be part of the capability. In addition, when the RB goes into and returns from plasma blackout, the simulation can be continued to determine the time required for the GPS receiver to acquire and establish navigational capability.

Keywords: Global Positioning System, re-entry, simulation, plasma propagation, missile

1. INTRODUCTION

This project's goal is to construct a hardware-in-the-loop Testbed for GPS receivers mounted on a Navy reentry body (RB). The Testbed must simulate the high velocities and consequent rapid changes in position and altitude expected for an RB to provide an adequate test of the GPS receivers. The GPS signal simulator[1] that will be used as a part of the Testbed is capable of these rapid updates, and also incorporates the attenuation and propagation delays encountered by the GPS signals as they pass through the ionosphere, a low density plasma whose electron density peaks near an altitude of 300 km. High energy radiation from the sun is largely responsible for ionization in this region. PSI's unique contribution to the simulator is to model the attenuation and delay caused by the plasma surrounding the RB as it reenters the lower atmosphere.

Beginning at an altitude of about 100 km (325 kft), a reentry body encounters significant and increasing atmospheric density. Shock heating, viscous energy transfer, and other processes raise the temperature of the atmosphere around the RB. Temperatures above 2000 K can occur, so that a small but significant amount of ionization occurs. The partially ionized gas is referred to as plasma. Atomic and molecular ions are factors of at least 2000 more massive than electrons, and are therefore less mobile. Their influence may be neglected for the most part. The free electrons can have a profound effect on the behavior of the plasma. Their effect on electromagnetic propagation will be considered here as it pertains to GPS signals received by the RB.

To test a GPS receiver under conditions simulating an RB re-entering the earth's atmosphere, the Testbed must be have models of a number of phenomena. First, it must create a realistic trajectory including the RB's position, velocity, and orientation. Based on the RB's trajectory, the Testbed needs to model the atmosphere surrounding the RB including the shock-heated plasma boundary layer and base region. The temperature of the boundary layer can be modeled fairly well without knowledge of the materials of which the RB is made. But the plasma electron density distribution is very sensitive to the chemical composition of the materials comprising the RB's outer covering, particularly the abundance of alkali metals such as sodium and potassium. The Testbed must also know the positions of the GPS satellite vehicles (SV)

* DFRANKEL1@rcn.com; phone 1 781 444-8442

on any given date at any time and must simulate their signals. The Testbed must model the gain pattern of the GPS receiver antenna(s). All of this processing must be done in real time to create an adequate test. Finally, the Testbed must compare the position determined by the receiver under test with the "true" position simulated by the Testbed and evaluate the receiver's accuracy.

In the Methodology section below, we develop the equations for electromagnetic wave propagation in a gaseous plasma and describe the architecture of the Testbed. In the Data section we show examples of the RB wake electron density distributions we have used and the RB motion model. In the Results section we compare these RB motion models with a GPS receiver's solution for its motion. The Conclusions section summarizes the lessons we have learned from constructing and using the Testbed.

2. METHODOLOGY

2.1 Propagation of electromagnetic waves in a plasma, neglecting collisions

The approach presented here follows closely the material developed in some published texts.[2,3,4] All of the results derive ultimately from Maxwell's Equations governing the electric and magnetic fields and their interaction with charged and neutral particles.

We are concerned primarily with the propagation of GPS signals through the plasma surrounding an RB as it reenters the Earth's atmosphere. As is the case for any electromagnetic wave, the GPS signal's properties may be modeled by considering its electric field. The electric field vector of an electromagnetic wave is usually modeled as a complex amplitude, $E_0(x, t)$ multiplied by a complex phase factor.

$$\vec{E}(\vec{x},t)=\vec{E}_0(\vec{x},t)\exp\left(i\vec{k}\cdot\vec{x}-i\omega t\right) \tag{1}$$

where $\vec{x}$ is the three dimensional position in space, the complex wave vector $\vec{k}$ has magnitude $2\pi/\lambda$, and ω is the angular frequency of the wave. In free space, $k_0^2c^2=\omega^2$, where c is the speed of light. The dependence of k on ω is called the dispersion relation. It plays a key role in describing propagation in a medium other than vacuum. For plane electromagnetic waves in a dielectric medium,

$$k^2=\frac{\omega^2\varepsilon}{c^2} \tag{2}$$

where ε is the dielectric constant. The dielectric constant and other important plasma properties depend on a parameter known as the plasma frequency, ω_p, given (in mks units) by

$$\omega_p=\left(\frac{10^6 n_e q_e^{\,2}}{\varepsilon_0 m_e}\right)^{\frac{1}{2}}, \tag{3}$$

where n_e is the electron number density (cm^{-3}), and q_e and m_e are the electron charge and mass, respectively. The plasma frequency is equal to the GPS L_1 carrier frequency (1575.42 MHz) for $n_e = 3x10^{10}$. The value of n_e for which $\omega_p = \omega$ is called the critical density, because if the density rises above this value, the wave will not propagate in the plasma.

For a cold, homogeneous, isotropic plasma, the dispersion relationship is

$$k_p^{\,2}=\frac{\omega^2-\omega_p^{\,2}}{c^2} \tag{4}$$

Note that if $\omega < \omega_p$, the wave vector is imaginary. This occurs above the critical value of n_c, corresponding to a wave that does not propagate. The corresponding high frequency dielectric constant is

$$\varepsilon = 1 - \frac{\omega_p^2}{\omega^2} \tag{5}$$

In an isotropic medium, the refractive index n is given by

$$\varepsilon = n^2 \tag{6}$$

Regardless of whether collisions are included, the phase velocity of a wave in a dielectric medium is

$$v_p = \omega / k \tag{7}$$

while the group velocity, the velocity at which energy and information are transmitted is

$$v_g = \frac{\partial \omega}{\partial k} \tag{8}$$

If collisions are neglected,

$$v_p = \frac{c}{\sqrt{1 - \omega_p^2/\omega^2}} \text{ and } v_g = c\sqrt{1 - \omega_p^2/\omega^2} \tag{9}$$

We may express these velocities in terms of refractive indices such that

$$n_{p,g} = c / v_{p,g} \, . \tag{9a}$$

In Figure 1 we plot the phase and group refractive indices, n_p and n_g respectively, of Eq. (9a), for $\omega = 2\pi \cdot 1575.42$ MHz, the GPS L_1 carrier frequency, as a function of n_c, the electron number density. Note that when $n > 3 \times 10^{10}$, $\omega_p > \omega$, and the velocities become imaginary. In this case, the wave does not propagate in the plasma. We show below that this result is modified by the effect of collisions.

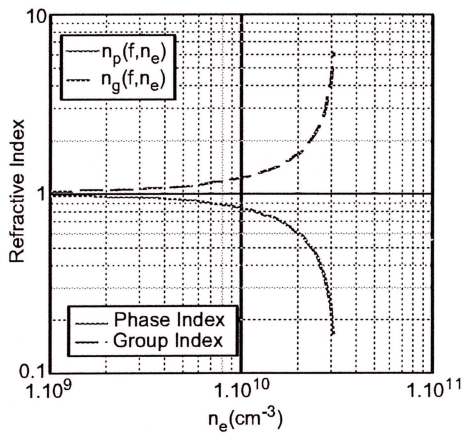

Figure 1. Phase (solid line) and group (dashed line) indices of refraction as a function of electron number density, n/cm^{-3}, for the GPS carrier wave frequency. The effect of collisions has been neglected.

2.2 Electromagnetic wave propagation in a plasma including collision effects

A major effect of electron collisions with other particles in the plasma is to allow absorption of energy from the wave. The wave vector becomes complex, and the wave amplitude diminishes as it propagates through the plasma. The simple model of the (angular) collision frequency is given by

$$\omega_c = n_n \sigma \sqrt{k_B \cdot T \cdot m} \tag{10}$$

where n_n is the number density of neutral species, σ is the collision cross section, k_B is Boltzmann's constant, and m is the electron mass. Near T = 1000 K, $\omega_c = 10^{11} p$, where p is the pressure in atmospheres.

When collisions are included, the dielectric constant may be expressed as

$$\varepsilon = 1 - \frac{X}{1 - iZ}$$

$$X = \left(\frac{\omega_p}{\omega}\right)^2 \qquad (11)$$

$$Z = \frac{\omega_c}{\omega}$$

As before, n, the refractive index, is the square root of the complex dielectric constant. The real and imaginary parts of n are μ and χ, respectively. The real part of n is related to the phase velocity of the wave as before, $v_p = c/\mathrm{Re}(n)$. A graph of Re(n) as a function of the electron number density is shown below in Figure 2. Note that phase velocities actually exceed the vacuum speed of light, but this does not violate Special Relativity because the phase does not carry energy or information. The real part of the refractive index reaches a minimum when the electron number density is such that $\omega_p = \omega_{GPS}$.

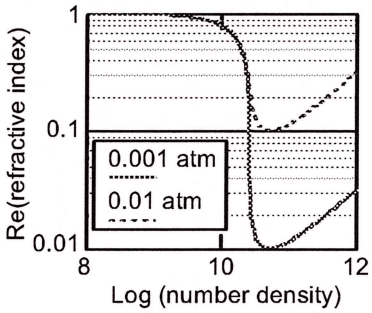

Figure 2. Real part of the refractive index vs. log number density (cm^{-3}) at the GPS frequency and the indicated pressure.

The absorption coefficient per unit length in the plasma is given by

$$\alpha = \frac{\omega}{c} i\sqrt{\varepsilon} \qquad (12)$$

or in other words, the absorption coefficient is ω/c times the imaginary part of the refractive index. A graph of the absorption coefficient as a function of log electron number density for several values of atmospheric pressure is shown in Figure 3. Note that absorption rises abruptly as the electron number density approaches the critical value, 3×10^{10} cm^{-3}.

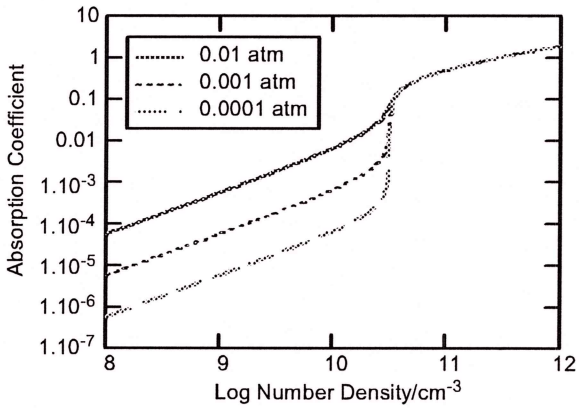

Figure 3. Absorption coefficient as a function of electron number density for three values of the ambient pressure.

Let us consider the case of a uniform slab of plasma having a constant electron density surrounded by vacuum. The reflection coefficient from its surface is given by

$$r = \left(\frac{(\mu - 1)^2 + \chi^2}{(\mu + 1)^2 + \chi^2}\right)^2 \qquad (13)$$

Figure 4 shows a semi-logarithmic plot of the single surface reflection coefficient as a function of electron number density for several values of the total pressure.

By combining the reflectivity and absorption results, we may derive an expression for the total transmission of electromagnetic energy through a uniform slab of plasma. The model will include reflective loss at the first surface, absorption loss through the plasma, transmission and internal reflection at the second surface, transmission back to the first surface, and so on. The result is

$$T = \frac{(1 - r)^2 \exp(-2\alpha L)}{1 - r^2 \exp(-4\alpha L)} \qquad (14)$$

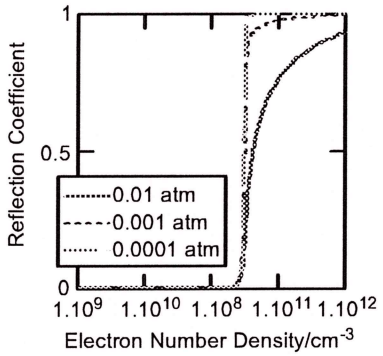

Figure 4. Plasma reflection coefficient as a function of electron number density for three values of the ambient pressure. Note the rapid rise in reflectivity as the number density approaches the critical value.

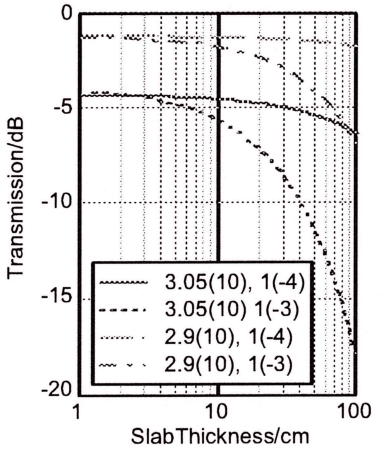

Figure 5. Plasma slab transmission in dB as a function of slab thickness for several combinations of electron number density and total pressure. In the legend, "3.05(10), 1(−4)" means an electron density of $3.05\text{x}10^{10}$ cm^{-3} and total pressure 10^{-4} atmosphere.

where r and α are the reflection and absorption coefficients, respectively, and L is the thickness of the plasma medium. If the reflection coefficients at the two boundaries are different, perhaps because of the presence of an antenna, then r^2 becomes $r_1 r_2$, etc. Figure 5 shows a graph of transmission as a function of plasma thickness for several combinations of electron number density and total pressure.

Attenuation, (absorption and reflection losses which eventually cause loss of signal lock), is one major effect of the reentry plasma on the usefulness of GPS for RBs. The other major effect is the pseudorange change. The plasma reduces the group velocity of the GPS signal through the plasma. The delay in GPS signal reception at the antenna translates into an additional range error. The group velocity may be expressed via the group refractive index,

$$n_g = \frac{1}{n_c}\left(1 + \frac{iZX}{2(1-iZ)^2}\right) \qquad (15)$$

where $n_c^2 = \varepsilon$ and the other symbols have been defined above. Figure 6 shows a graph of n_g for two values of the total pressure.

When the GPS signal traverses the plasma surrounding the RB, its velocity is reduced, as shown in Figure 6, above. The additional time required for the signal to reach the GPS antenna is processed into a change in pseudorange, contributing to the error in RB position. The pseudorange change attributable to the RB plasma is

$$dr = (n(L) - 1)dL$$

where dL is a differential length over the ray path through the plasma. Similarly, the attenuation in signal power is given by $dP = -\alpha(L)PdL$. To illustrate the magnitude of these effects, we will initially approximate the integrals by treating n and α as constants over the path. Figure 7 shows a plot of pseudorange change vs transmission for a 10 cm path. The plasma electron density varies from 10^9 (at the top of the trace) to $6.3\text{x}10^{10}$ (at the bottom) in this figure. At higher electron densities, the pseudorange change varies very little, while the transmission continues to fall precipitously.

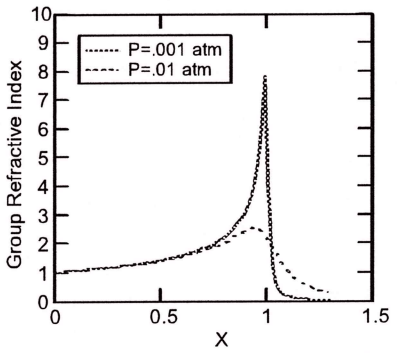

Figure 6. Group refractive index as a function of $X = (\omega_p/\omega)^2$ for two values of the total pressure. Above X = 1, the index becomes less than unity, but the wave does not truly propagate. Therefore, no violation of Special Relativity occurs.

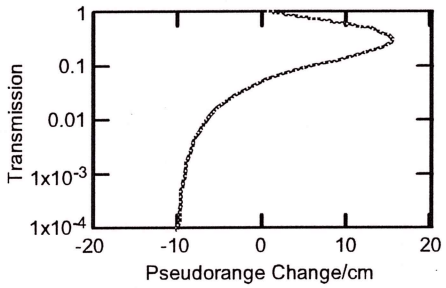

Figure 7. Transmission vs. pseudorange change for a 10 cm thick plasma slab at total pressure 0.01 atm. At the top of the trace, $n_e = 10^9$. At that density, transmission ≈ 1 and pseudorange change ≈ 0. At the bottom of the plot, $n_e = 6.3\text{x}10^{10}$. This is greater than the critical density, and the electromagnetic wave no longer propagates but rather is reflected from the first surface.

2.3 Testbed architecture

Our approach to creating the GPS signals is to employ the CAST Navigation simulator. Our Testbed must therefore communicate to the CAST simulator the date and time of the test and all of the RB trajectory properties that affect the received signal. This is be an iterative process. The date and time of the test first must be transmitted to the CAST simulator. The simulator responds by transmitting to the Testbed the almanac data of the satellites at that time. Then the Testbed must calculate the positions of the SVs and all of the other parameters affecting transmission of the GPS signals to the RB: the antenna gain pattern, RB orientation, and plasma electron density distribution. Given the then known positions of the SVs and the RB, the line of sight (LoS) from the RB to each SV can be calculated. By combining the LoS geometry with the antenna gain pattern, with the plasma electron density distribution, and with the electromagnetic propagation equations, the Testbed can estimate the attenuation and pseudorange change for each SV's signal. The Testbed then transmits these data to the CAST simulator. The CAST simulator uses the relative positions of the RB and the SVs to choose the 10 best SVs to use. The CAST Simulator then transmits the simulated GPS signals from these 10 best SVs to the GPS receiver under test.

Figure 8 shows the overall architecture of the GPS Receiver Testbed, including the GUI and the main modules of the testbed, the CAST Navigation simulator, the trajectory module, and the LOS Effects module, which calculates attenuation and pseudorange change.

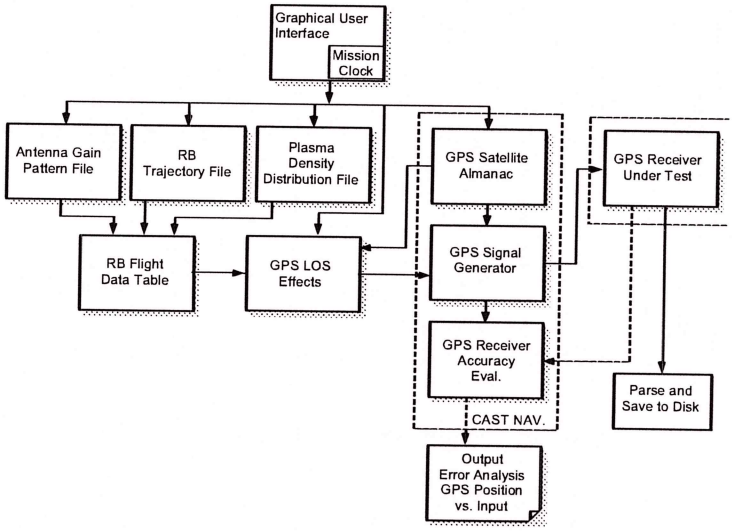

Figure 8. GPS Receiver Testbed Top Level Design. User input to the GUI chooses the date and time of the simulated mission and the source of the trajectory and flow field data, i.e. whether the default missions or one that is user-supplied. These data are added to the Flight Data Table, which is a central resource for describing the mission and conducting the simulation.

As mentioned in Subsections 2.1 and 2.2 above, the plasma surrounding the RB during atmospheric re-entry affects transmission of the GPS signals in two important ways: attenuation and pseudorange change, which were shown to be the result of the plasma's complex refractive index. Calculating these effects is the responsibility of the GPS LoS Effects Module, as shown in Figure 9.

3. DATA

3.1 Trajectory data

Because the simulation is so complicated, a stepwise approach was adopted for evaluating the Testbed's performance. First, a motionless RB case allowed us to isolate any issues associated with the GPS simulator without the complications of a moving RB or plasma effects. To simplify interpretation of the results, we placed the RB over earth locations such as the north and south poles and the equator. When the stationary cases were complete,

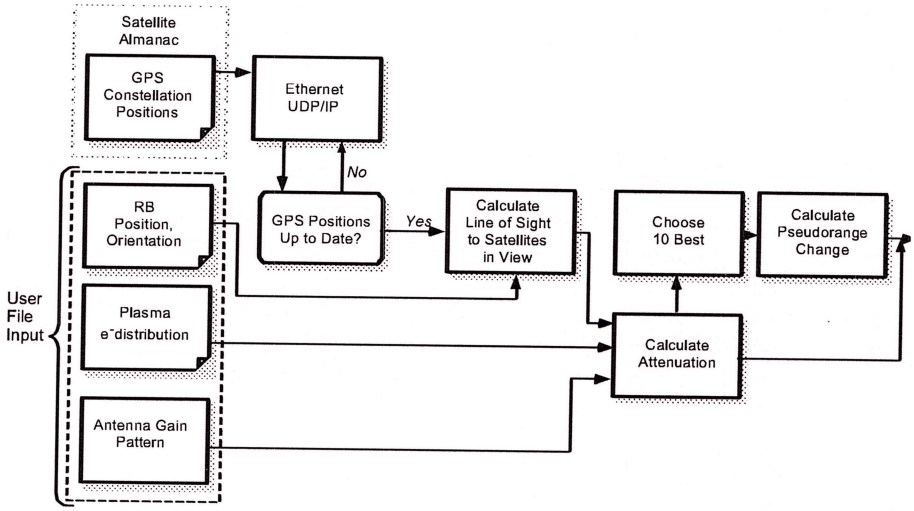

Figure 9. GPS LoS Effects Module. In this module, the test bed calculates the LoS from the RB to each SV. Transmission through the estimated electron density distribution and the antenna gain are calculated along the line of sight to each SV.

we then introduced trajectories typical of re-entry conditions.[5] Similar trajectories were used both with and without including the effects of plasma propagation. Initial conditions for these cases are given in Tables 1 and 2 below. Gamma is the angle between the velocity vector and the local horizontal.

Table 1. Initial Conditions for Trajectory Cases Neglecting Plasma Effects

Parameter	Value	
Case	Trajectory 1	Trajectory 2
Date	19 Oct 97	19 Oct 97
UTC	0 h: 0 m: 20 s	0 h: 0 m: 20 s
Trajectory file	kepler-1030	case_23.trj
Antenna	dsf.ant	dsf.ant
SV motion	ON	ON
RB motion	ON	ON
Plasma effects	OFF	OFF
Attitude mode	EULER	EULER
Initial position	66.7 E; 36.2 N; 1,161 km alt.	135 W; 65 N; 3800 kft alt.
Initial speed	2.5 km/s	1.89 km/s
Initial azimuth	49.8°	180°
Initial gamma	-55.8° (ascending)	-60° (ascending)

Table 2. Initial Conditions for Trajectory Cases Including Plasma Effects

Parameter	Value	
Case	Trajectory 1	Trajectory 2
Date	19 Oct 97	19 Oct 97
UTC	0 h: 0 m: 20 s	0 h: 2 m: 0 s
Trajectory file	case_23.trj	case_23.trj
Antenna	dsf.ant	dsf.ant
SV motion	ON	ON
RB motion	ON	ON
Plasma effects	ON	ON
Attitude mode	EULER	EULER
Initial position	135 W; 65 N; 3800 kft alt.	135 W; 65 N; 3800 kft alt.
Initial speed	1.89 km/s	1.89 km/s
Initial azimuth	180°	180°
Initial gamma	-60° (ascending)	-60° (ascending)

3.2 Base region electron density distributions

While boundary layer flows can be calculated with relative ease, most Navy re-entry bodies have the GPS antenna on the base of the RB. Calculating the electron density distribution in this very complicated flow region was beyond the scope of this project. We instead used published results[6] of plasma calculations for a reentry body trajectory at 35, 40, and 45 kft altitudes. A 10 by 20 point overlay grid was placed on the density contour maps and the plasma density at each point was read from the graph. These points were then entered into a text file in the format required for electron density data: x (axial) distance, y (radial distance from x axis), z (0), and the density. Cylindrical symmetry is assumed for these data, hence z distance is redundant. The z dimension is nevertheless retained in the file format to allow for unsymmetrical distribution cases. Typical electron density calculations are shown in Figure 10.

4. RESULTS

4.1 Stationary cases

The results of the stationary cases may be illustrated by the results shown in Figure 11. In this simulation, the RB was located directly over the north pole beginning at 01 h UTC. As is evident from the figure, almost 10 minutes elapse before the GPS receiver locks onto the GPS signal. Once it has locked on, the error in latitude and longitude are less than 1 meter. The arrow indicates one anomaly that is often observed. Occasional discontinuities in the time base occur, namely, the time reported by the receiver jumps back about ten seconds. It is not known at this time whether the GPS Simulator or the GPS receiver is responsible for the discontinuity. Probably the best way to find out is to use a different receiver. The other anomaly illustrated by the figure is the occurrence of latitude values greater than 90 degrees. Differences in receiver and simulator altitude are 25 m or less. The larger difference is probably due in large part to the different geoid models used by the simulator and the receiver.

4.2 Moving RB trajectories neglecting plasma effects

The tests with stationary targets described above allowed us to confirm that the system functions properly aside from occasional peculiarities in the receiver's output. We then turned our attention to tests using RB re-entry trajectories. In

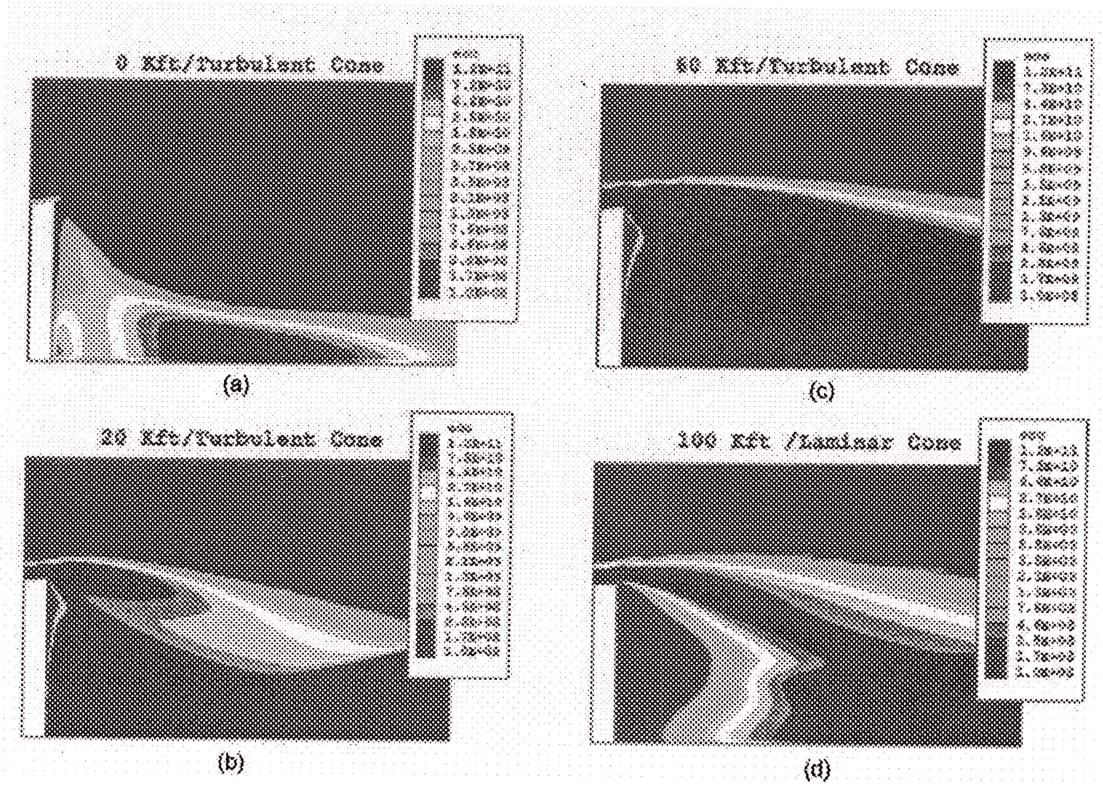

Figure 10. Base region electron density contours for an RB at four altitudes.

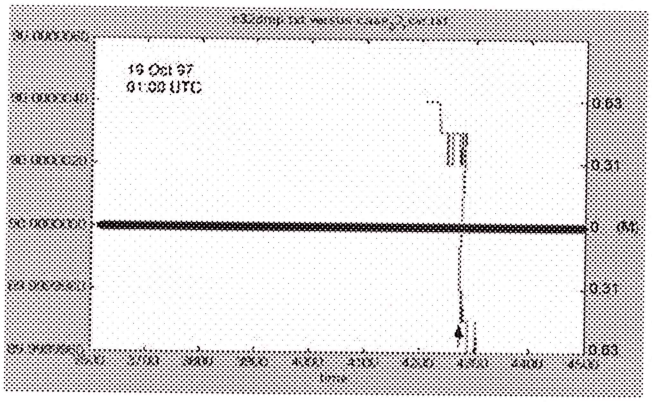

Figure 11. Recorded latitude vs. time for a static antenna over the North Pole. The thick line is the CAST Simulator's output, which we will refer to as the "true" position. The thin line is the "Golden Receiver's" solution for its position. Note that 600 seconds elapsed before the receiver locked on to the GPS signal and achieved a navigation solution. After lock-on, the difference between the receiver's position and the "true" position is very small. The arrow indicates a discontinuity in the time base. Note that the receiver reports latitudes greater than 90 degrees.

keeping with our approach of testing new features one at a time to help isolate any problems that might arise, we first ran re-entry tests neglecting plasma effects. Figure 12 shows a plot of longitude vs. time for Trajectory 2 in Table 1. In this case, the GPS receiver locks on after only 160 s, which is typical of all of the trajectories tested. The GPS receiver solution follows the true trajectory very closely until 534 s, at which time a discontinuity in the time base occurs. The receiver stays locked on until the trajectory ends at 926 s. Figure 13 is a plot of the latitude vs. longitude for this same case. Since no kink appears in this plot, it is clear that the only discontinuity in the receiver's output is in the time stamp.

4.3 Trajectories including plasma effects

The tests with re-entering targets described above allowed us to confirm that the system functions properly with RBs in motion, aside from repeatable discontinuities in the receiver's output time base. We then turned our attention to testing the plasma transmission effects modules. We used the initial re-entry trajectory conditions listed above in Table 2. The two cases including plasma effects differ only in the starting UTC time: Trajectory 2 begins 100 s later than Trajectory 1. The delay was introduced to help understand the nature of the time base discontinuity observed in prior tests.

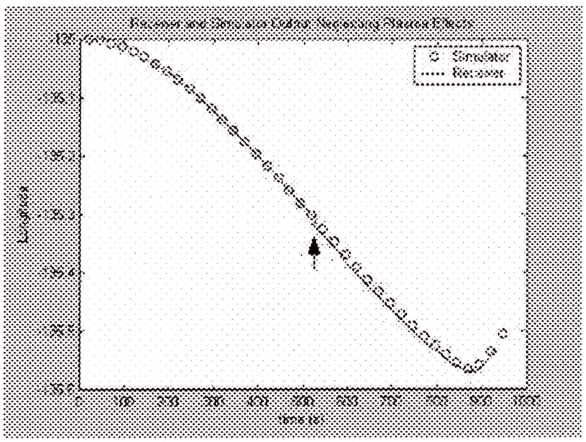

Figure 12. Longitude vs. time for Trajectory 2 shown in Table 1. The open circles are the CAST simulator's output. The solid line is the receiver's navigation solution. Only every fiftieth point of the simulator's output has been plotted. The CAST Simulator's output begins at t = 20 s. GPS receiver lock-on occurs near 170 s. The true longitude and the receiver's solution are very close until the time discontinuity indicated by the arrow near t = 534 s. The GPS receiver maintains lock until the trajectory ends at t = 926 s

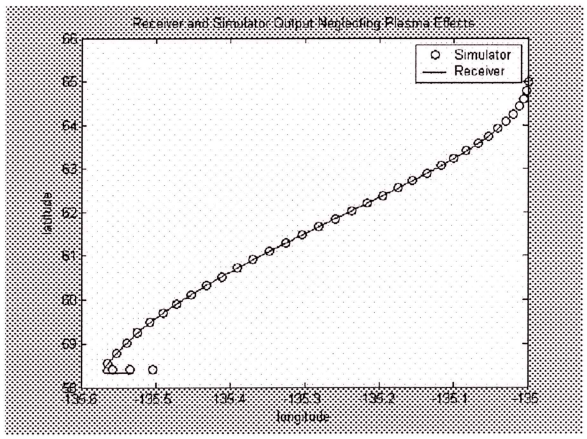

Figure 13. Latitude vs. longitude for Trajectory 2 shown in Table 1. The open circles are the CAST simulator's output. The solid line is the receiver's navigation solution. Only every fiftieth point of the simulator's output has been plotted. The CAST Simulator's output begins at t = 20 s. GPS receiver lock-on occurs near 170 s. The true longitude and the receiver's solution are very close. The GPS receiver maintains lock until the trajectory ends at t = 926 s.

A plot of the longitude as a function of time for this case is shown in Figure 14. The same time base discontinuity as in previous cases is apparent at t = 534 s. A plot of latitude vs. longitude is shown in Figure 15. There are no kinks in the plot in Figure 15, showing clearly that the receiver's error is only in the time base. The essential difference between the results with and without the plasma effects can be seen by comparing Figure 14 to Figure 12. When the plasma effects

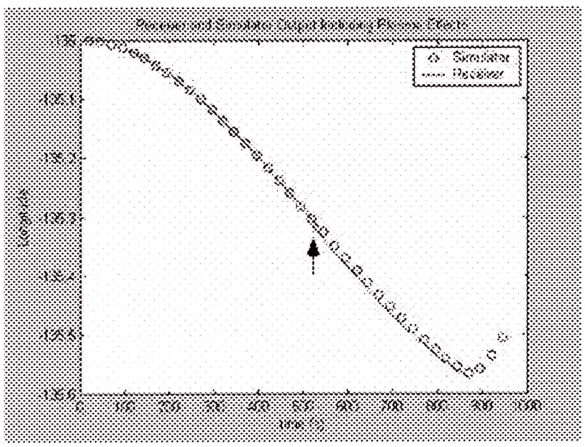

Figure 14. Longitude vs. time for Trajectory 1 listed in Table 2. The open circles are the CAST simulator's output. The solid line is the receiver's navigation solution. Only every fiftieth point of the simulator's output has been plotted. The CAST Simulator's output begins at t = 20 s. GPS receiver lock-on occurs near 100 s. The true longitude and the receiver's solution are very close aside from the time discontinuity indicated by the arrow near t = 534 s. The receiver loses lock at t = 869 s.

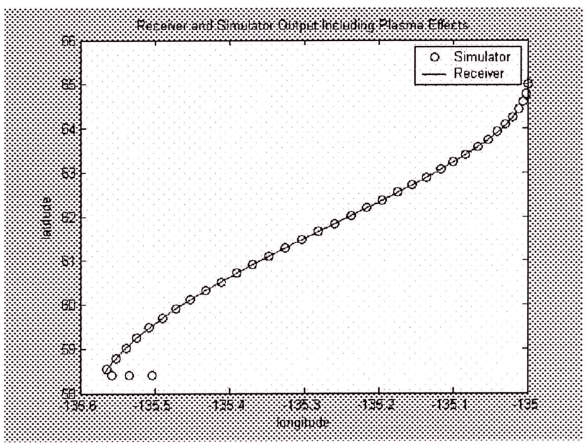

Figure 15. Latitude vs. Longitude for Trajectory 1 listed in Table 2. The open circles are the CAST simulator's output. The solid line is the receiver's navigation solution. Only every fiftieth point of the simulator's output has been plotted. The CAST Simulator's output begins at t = 20 s. GPS receiver lock-on occurs near 100 s. The true longitude and latitude and the receiver's solution are very close throughout the trajectory. The receiver loses lock at t = 869 s at an altitude near 24 km, rather than at the end of the trajectory, as it did when plasma attenuation effects were neglected.

are included, the receiver loses lock before the end of the trajectory at an altitude near 24 km. Loss of lock is precisely the behavior expected when plasma attenuation occurs. Results using Trajectory 2 in Table 2 were very similar. Notably, the time base discontinuity still occurs at t = 534 s, even when the trajectory begins at t = 120 s rather than t = 20 s. Therefore the discontinuity must be associated with the time of day, rather than the duration of the trajectory.

The results discussed above may be summarized as follows

- Achieving GPS lock can take several minutes.
- GPS latitude and altitude solutions are accurate to within 1 m or less.
- Altitude discrepancies are larger than latitude and longitude errors. The differences are close to what might be expected for the different earth geoid models used by the CAST simulator and the receiver.
- Time stamp discontinuities occur in the receiver at certain times of day for both stationary and moving receivers.
- Oddities can occur in a receiver's output, at least for special cases such as latitude = 90.
- The trajectory code used must be validated during re-entry.
- When plasma effects are neglected, GPS navigation solutions are maintained until the end of the trajectory.
- When plasma effects are included in the simulation, GPS navigation solutions end at altitude = 24 km.

5. CONCLUSIONS

Our primary conclusion from the work performed to date is that the GPS Receiver Testbed is now ready for thorough testing. More detailed conclusions we draw from the results described above may be stated as follows.

- Ethernet communication between the Testbed and the CAST Simulator works correctly to transmit or receive messages containing almanacs, trajectory data, and loss and delay data representing plasma propagation effects.
- GPS receiver control instructions are being sent properly by the Testbed and receiver position solution data are being received and parsed properly.
- The Testbed's graphical user interface functions as it was designed to give the user control over the simulation.
- Using trajectory and plasma data files created off-line gives the user a great deal of flexibility in creating a simulation.

ACKNOWLEDGEMENTS

The authors wish to thank Frank J. Regan, formerly of the US Naval Surface Warfare Center, Dahlgren, for providing us with a MATLAB script for calculating the RB trajectories used here. This work was supported by US Navy Phase II SBIR contract N00178-02-C-3015.

REFERENCES

1. CAST Navigation, LLC, 900 Technology Park Drive, Billerica, MA 01821
2. Krall, N. and Trivelpiece, *Principles of Plasma Physics*" San Francisco Press, 1986
3. Budden, K.G., *Radio Waves in the Ionosphere*, Cambridge University Press, 1961
4. Ruck, G.T., Barrick, D. E., Stuart, W.D., Krichbaum, C.K., *Radar Cross Section Handbook, Volume 2*" Plenum Press, New York, 1970
5. Frank J. Regan and Satya M. Anandakrishnan, *Dynamics of Atmospheric Re-Entry,* AIAA Education Series, J. S. Przemieniecki series editor-in-chief, American Institute of Aeronautics and Astronautics, Inc., Washington, DC, 1993
6. Meyer, J.W. and Thompson, T., "Analysis of Plasma Results from the Reentry Flap Technology Experiment," 1998 AIAA Missile Sciences Conference, Monterey, CA, November 17-19, 1998